AIAA JOURNAL
Vol. 45, No. 5, May 2007

Jet Impingement Tone Suppression Using Powered Resonance Tubes

Shekhar Sarpotdar,* Ganesh Raman,† and S. D. Sharma‡
Illinois Institute of Technology, Chicago, Illinois 60616
and
Alan B. Cain§
Innovative Technology Applications Company, LLC, Chesterfield, Missouri 63006-6971

DOI: 10.2514/1.15818

This work is an experimental study of high subsonic jet impingement tone suppression. We begin by documenting the characteristics of the impingement tone for various Mach numbers and standoff (nozzle exit to ground plate) distances. The results revealed frequency staging and the presence of two types of impingement tones. A novel feature of our work is the use of four miniature high-frequency actuators known as powered resonance tubes that were located circumferentially around the main jet nozzle. The powered resonance tubes were capable of producing high amplitude acoustic excitation over a range of frequencies, up to 17.5 kHz. Our target excitation frequency range was about 3–5 times that of the natural flow instability. Using high-frequency excitation, tonal suppression levels as high as 20 dB and broadband suppression levels as high as 5–10 dB were obtained. The mass addition rate from the powered resonance tubes was of the order of 2% of the mass flow rate from the main jet. Mass flow reductions could be obtained under conditions when the powered resonance tube resonated strongly. Our results suggest that appropriately designed miniature powered resonance tube actuators have potential for use in flow control applications.

Nomenclature

a_∞	=	speed of sound corresponding to the freestream conditions
C_1, C_2	=	correction factors for the main jet velocity and the acoustic velocity, respectively
D	=	main nozzle exit diameter
f	=	frequency of the acoustic wave
h	=	standoff distance between the nozzle exit and ground plate
M	=	Mach number
n	=	number of the impingement stage
p	=	phase shift associated with acoustic wave reflection
u	=	flow velocity
λ	=	acoustic wavelength

Subscripts

j	=	main jet properties
PRT	=	powered resonance tube

I. Introduction

WHEN a high-speed freejet of air is directed normally onto a flat plate and the flow Mach number exceeds about 0.6, it gives rise to discrete tones of very large amplitude, referred to as jet impingement tones [1]. This phenomenon poses many problems when it arises in practical situations [2–4]. For example, in laser cutting, it is a common practice to remove the molten mass of metal with the help of a high speed jet of air. In this application, the quality of the cut depends on the oscillatory behavior of the jet. A stable jet, free of any impingement tones, results in deeper, cleaner, and straighter laser cuts. Thin glass sheets are prone to cracks when the sheets are tempered by a jet of cold air producing impingement tones. One method of surface coating, known as cold gas dynamic spray coating, is carried out by blasting fine grain metal powder directly onto the surface that is to be coated using a high velocity jet of air. In this application, the quality of the surface finish is largely dependent on the stability of the jet. An unstable jet deteriorates the surface finish. Another application, which is the motivation of the present work, is for short takeoff vertical landing (STOVL) aircraft. When the aircraft is in close proximity to the ground, the exhaust plumes from the engines hit the ground and generate impingement tones. Loss of lift, sonic fatigue, and ground erosion are some of the problems caused by the impingement of hot plumes from the engines while the STOVL aircraft is in the hovering mode close to the ground.

Figure 1 shows a schematic of the feedback loop that involves the generation of jet impingement tones. The sequence of events in the feedback loop is as follows: the interaction of the unsteady flow with the ground gives rise to pressure disturbances. These disturbances then travel upstream and excite the shear layer at the lip of the nozzle. This periodic excitation strengthens the instabilities in the shear layer and thus produces large scale coherent structures. When these large scale structures impinge on the ground, the sound generation mechanism is further intensified, thus completing the feedback loop and producing high intensity discrete frequency tones that are known as impingement tones. In the present experiments, the amplitude level of the impingement tone is measured to be as high as 145 dB at $3.2D$ from the main nozzle. The frequency of the tone depends on a number of parameters, viz., Mach number of the jet, the standoff distance between the nozzle exit and the ground plate, and the exit diameter of the nozzle.

There are several methods of flow control that are relevant to the suppression of the impingement tone. Sheplak and Spina [5] used a high speed coaxial flow to shield the shear layer of the main jet from

Presented as Paper 0797 at the AIAA Aerospace Sciences Conference, Reno, NV, 10–14 January 2005; received 8 July 2005; revision received 18 October 2006; accepted for publication 20 October 2006.

*Graduate Student.
†Associate Dean for Research, Associate Fellow AIAA.
‡Visiting Professor, Permanent Address: Indian Institute of Technology, Mumbai, India.
§President, Associate Fellow AIAA.

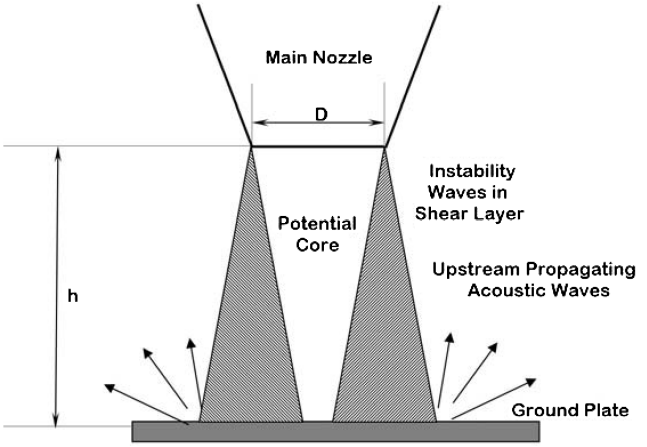

Fig. 1 Schematic of the impingement tone feedback mechanism.

the disturbance waves. This method suppressed the broadband noise levels by more than 10 dB and also completely suppressed the impingement tone, but at the cost of large mass flow rates reaching up to 20–25% of the main jet. Recently, Alvi et al. [6] employed a circular array of microjets around the periphery of the main jet that resulted in a reduction of 8 dB in the overall sound pressure level (OASPL).

Depending on the relation between the forcing frequency of the excitation and the initial frequency of the instability, active flow control (AFC) can be subdivided into two classes [7]: AFC-I and AFC-II. AFC-I involves the use of relatively low-frequency unsteady forcing to excite instability waves in laminar flows, or the large scale structures in turbulent flows. This technique has been used extensively in the past decade [8]. The second class, AFC-II, which has been developed more recently, involves forcing of the shear layer at relatively high frequency. Wiltse and Glezer [9] were the first to demonstrate the efficacy of high-frequency excitation of the turbulent shear layer. Their measurements showed that high-frequency excitation in the transitional region of the shear layer inhibits the growth rate of large scale structures. Cain et al. [10] numerically showed that the magnitude of suppression of the turbulent kinetic energy increased monotonically when the magnitude of forcing exceeded a threshold level. For a given forcing energy, the largest reduction in the turbulent kinetic energy was achieved at forcing frequencies that were 2–3 times the neutral frequency determined from the linear stability theory. For the impingement tone to occur, the formation of large scale turbulent coherent structures is important. Because high-frequency forcing of the shear layer in the transition zone inhibits the formation of large scale structures, one can expect that a high-frequency acoustic signal from the powered resonance tube (PRT) would suppress the impingement tone.

The PRT, also referred to as a Hartmann whistle [11], is an actuator that is based on aeroacoustic operating principles [12,13]. It consists of a cylindrical tube that is open at one end and closed at the other with a slotted opening in the middle. A supersonic underexpanded jet is directed through the open end of the tube in order to generate a resonant excitation within the tube. Past investigations [14–16] have demonstrated that the PRT can generate resonant excitation over a wide range of frequencies (3–18 kHz) with significantly high amplitudes of the order of 150 dB. These characteristics fulfill the basic requirements of a high-frequency acoustic actuator and make the PRT a suitable device to be used in AFC applications. However, it is surprising that the potential of this incredibly simple device has not been fully exploited. Murugappan and Gutmark [17], Kastner et al. [18], Raman and Kibens [19], and Raman et al. [20] have investigated the application of PRTs for controlling high speed flows. The use of the PRT and other active flow control actuators is also described in a review paper by Raman and Cain [21].

The present investigation addresses a practical problem of a high intensity tone generated by a high speed jet impinging normally onto a ground plate. Here, our focus is to understand the behavior of a high subsonic jet produced by a nozzle and directed normally onto a ground plate from varying distance, and to then suppress the dominant impinging tone by means of high-frequency excitation using miniature PRTs through systematic experiments.

II. Experimental Apparatus

Figure 2 shows a schematic of the experimental setup. The convergent conical nozzle (referred to as the main nozzle) has an exit diameter D of 31.75 mm (1.25 in.) and a contraction ratio of 2.56 over a linear profile and a taper angle of 7 deg. The main nozzle is supplied

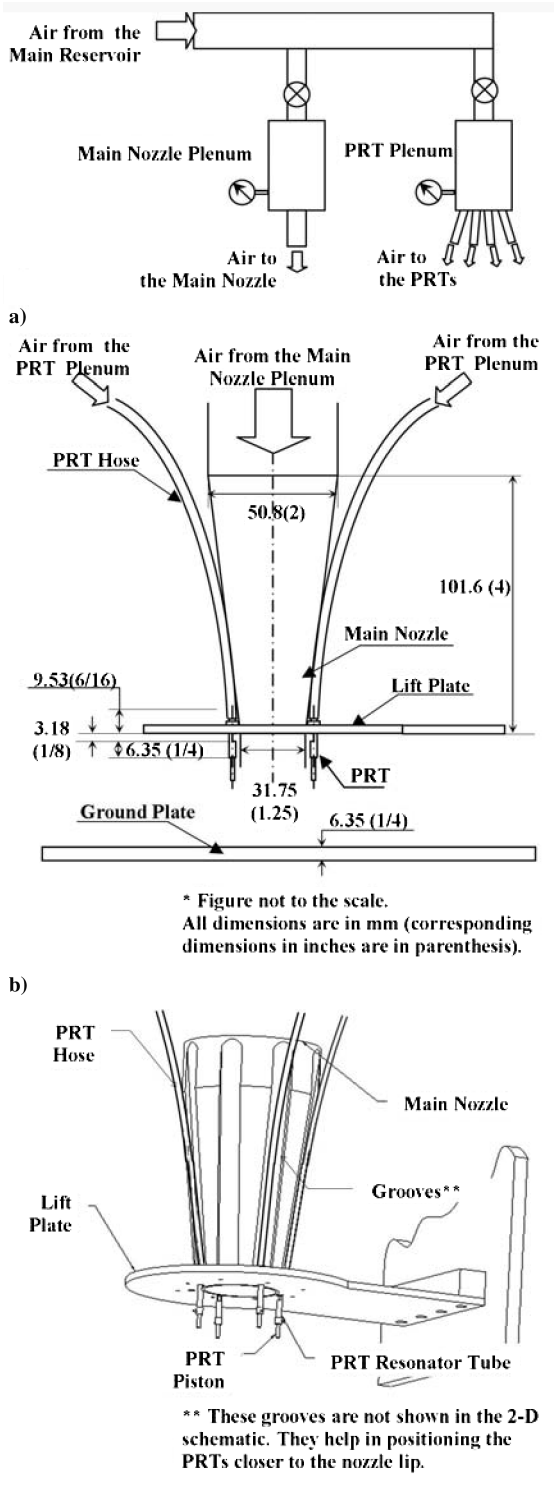

Fig. 2 Experimental setup a) air supply arrangement; b) 2-D schematic; and c) 3-D view.

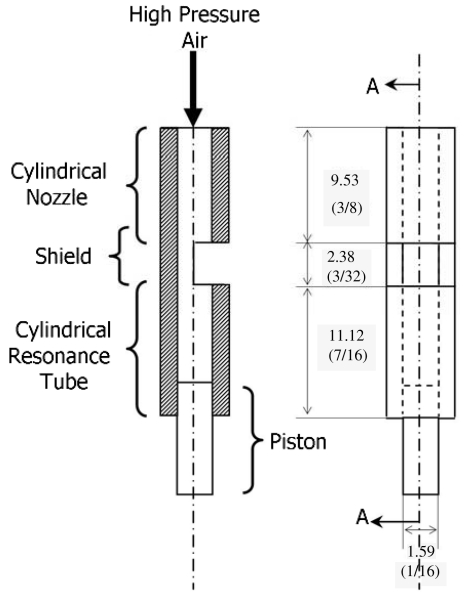

Fig. 3 Geometric details of the powered resonance tube (PRT). All dimensions are in mm (corresponding dimensions in inches are in parentheses).

with air from a cylindrical plenum that has a diameter of 152.4 mm (6 in.) and a length of 914.4 mm (36 in.). A circular plate, referred to as the lift plate, having a diameter of 101.6 mm (4 in.), is mounted flush with the main nozzle exit. This plate is meant to simulate the body of an aircraft. The main nozzle exhausts vertically downward, above a square ground plate which can be traversed up or down to vary the standoff distance from the lift plate. The ground plate is made out of a 6.35 mm (0.25 in.) thick aluminum sheet cut to the size of 685.8×685.8 mm. It is sufficiently large compared to the main nozzle diameter to serve as the ground when the jet impinges onto it at its center.

Figure 3 shows the design of the PRT that is used in the present experiments. High pressure air is fed through the cylindrical nozzle to generate a supersonic jet of air at the open end of the tube. The closed end of the tube incorporates a piston to adjust the depth of the resonator tube and consequently the frequency of the resonance. A shield, which is located between the ends of the tubes, is used to improve the directivity of the resonant excitation. Four such PRTs with an internal diameter of 1.59 mm (0.0625 in.) are mounted on the lift plate along the lip of the main nozzle with equal azimuthal spacing. The net area of all the four PRTs constitutes just 1% of the nozzle exit area. The shields of the PRTs direct the resonant excitation toward the axis of the main jet. Air from a plenum chamber, with the dimensions 76.2 cm (3 in.) in diameter and 91.44 cm (36 in.) in length, is supplied through individual flexible tubes to the PRTs. To ensure the straightness of these tubes they are held firmly inside equally spaced longitudinal grooves provided on the outer wall of the main nozzle. It is to be noted that the main jet plenum chamber and the PRT plenum chamber both draw air from a common reservoir with maximum storage pressure being up to 15 atm. The air supply to these plenum chambers is regulated through separate control valves such that their pressures can be maintained independently.

The stagnation pressures in the plenums of the main jet and PRTs are measured using Setra, model 204, pressure transducers. The impingement tone frequency is measured with a B&K, model 4393, microphone that is located at a distance of $3.2D$ from the main nozzle. The data are sampled at a rate of 500 kHz for a period of 1.6 s. The microphone signal is bandpassed through a fourth order analog Bessel filter to avoid aliasing. The high pass frequency is 10 Hz, and the low pass frequency is 100 kHz.

In the data analysis, the time series of the measured stagnation pressure of the main jet is subdivided into five segments. The mean values of these segments varied by the order of 4.20×10^{-3}NPR (nozzle pressure ratio) (0.1 psi). The measured microphone data that corresponded to the segment of stagnation pressure whose mean value is closest to the desired stagnation pressure is used in the subsequent data analysis.

III. Results and Discussion

A. Characteristics of the Impingement Tone

To characterize the salient features of the impingement tone such as tonal frequency, tonal sound pressure level (SPL), and OASPL, the main jet was run at a Mach number $M_j = 0.86$, with standoff distances h/D varying in the range of 1.6–3.3 in increments of 0.1. At each standoff distance, measurements were made with and without the lift plate.

As described earlier, for the impingement tone to occur, the upstream traveling acoustic waves must strengthen the nascent instability waves at the nozzle exit to form coherent structures in a periodic fashion. The sum of the time taken by the coherent structures to travel from the nozzle lip to the ground plate and the time taken by the acoustic waves to travel from the ground plate to the nozzle lip constitutes the time period of the corresponding impingement tone frequency. Mathematically the above statement is equivalent to the phase locking formula proposed by Powell [14], which is as follows:

$$\frac{1}{f} = \frac{1}{n+p}\left[\frac{h}{C_1 u_j} + \frac{h}{C_2 a_\infty}\right] \tag{1}$$

where the main jet velocity correction factor C_1 is used to obtain the convective velocity of the coherent structures that move in the shear layer at relatively lower speed. Empirically the value of C_1 has been found to lie between 0.55 and 0.7 and is expected to change along the jet length due to stagnation effect as the ground plate is approached. In the present work, the value of $C_1 = 0.6$ yielded the closest match with the above equation. The acoustic waves are assumed to travel in the region exterior to the jet; hence, C_2 is assumed to be 1. The phase shift p which is associated with the reflection of the acoustic waves from the ground plate is arbitrarily assumed to be zero.

Figure 4 compares the experimentally measured impingement tone frequencies for various values of standoff distance with those predicted by the phase locking formula [Eq. (1)]. A very short vertical error bar indicates excellent consistency in obtaining the frequency of the impingement tones. If we compare Figs. 4a and 4b one may observe that the effect of the lift plate is evident only for shorter standoff distances ($h/D < 2.4$). We believe that the presence of the lift plate facilitates a situation similar to the plane of symmetry between the source and its image that would enhance the pressure field in the shear layer and force the coherent structures to organize in the scale appropriate to a lower mode. A significant jump observed in the frequency from around 7 to 4 kHz for $h/D < 1.8$ seems to support this viewpoint. In Fig. 4b one may observe that for $h/D < 2.3$ the experimental data closely follow the phase lock curve with $n = 2$. To maintain the same mode, for increasing standoff distance, the scale of the coherent structures and consequently the wavelength of the instability waves must increase. However, there is a maximum limit on the wavelength of the instability waves that a jet can support. When the standoff distance is increased beyond a threshold value the jet fails to support the long instability waves. As a result the wavelength of the instability waves is shortened, with the corresponding jump in the impingement tone frequency. The present results clearly exhibit this phenomenon of mode jump or staging at $h/D = 2.3$.

Figure 5 shows the variation, with respect to the standoff distance, of the OASPL and tonal SPL without the lift plate (Fig. 5a) and with the lift plate (Fig. 5b). In general, the lift plate is seen to enhance both the OASPL and the tonal SPL. From a closer examination of Figs. 5a and 5b it appears that although the lift plate plays an important role in the phase locking, particularly for $h/D < 2.4$, it does not enhance the impingement tone SPL. However, the OASPL registers higher values indicating a significant rise in the total energy. A difference in magnitudes of impingement tone SPL and OASPL is seen to reach up to 10 dB in the regions of shorter standoff distance. However, this

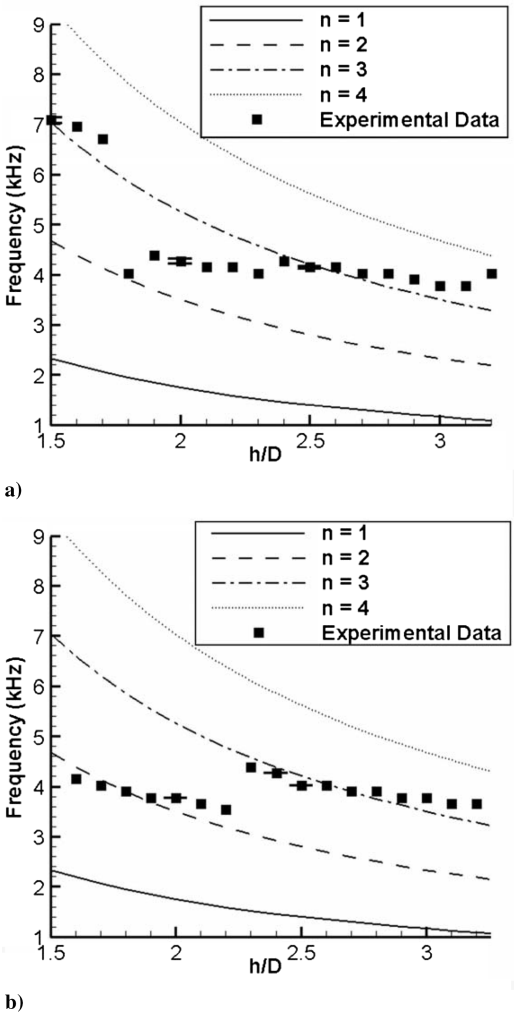

Fig. 4 Impingement tone frequency staging obtained at $M_j = 0.86$ for two cases: a) without lift plate and b) with lift plate.

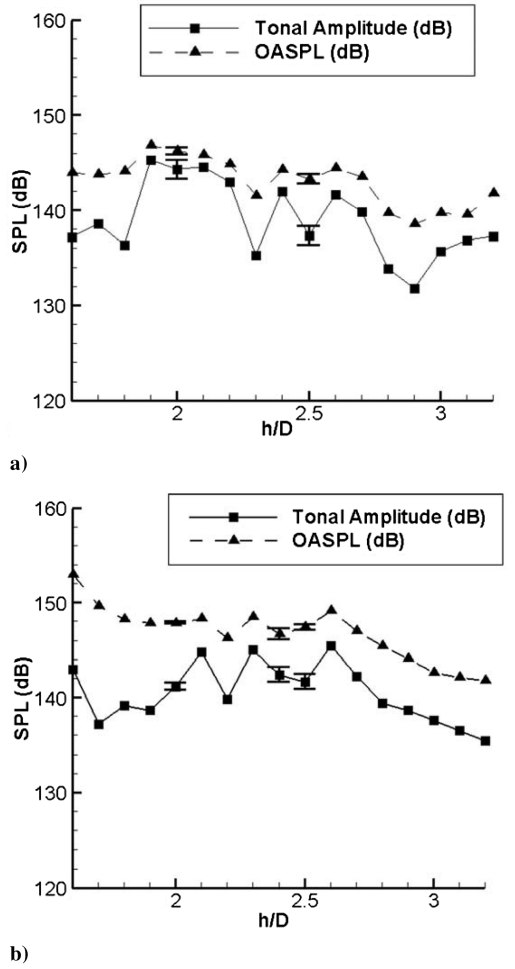

Fig. 5 Variation of the impingement tone amplitude and OASPL with a stand of distance at $M_j = 0.86$. a) Without lift plate and b) with lift plate.

difference is within 6 dB for larger standoff distances suggesting that most of the energy is contained in the narrow frequency band. It is also noted from Fig. 5b that beyond $h/D = 2.6$ as the standoff distance is increased, it results in consistent reduction in both the tonal SPL and the OASPL. Because the measured and predicted frequencies are found to be in good agreement (Fig. 4b), the subsequent experiments to examine the jet impingement tone suppression using PRTs are conducted with the lift plate.

The variation of the tonal frequency with the main jet Mach number at a constant standoff distance is shown in Fig. 6. In Fig. 6a the standoff distance is $h/D = 2.4$ and the jet Mach numbers are in the range of 0.78–0.91. In Fig. 6b, the standoff distance is $h/D = 3.2$, whereas the jet Mach number is varied between 0.81 to 0.94. For the $h/D = 2.4$ case (Fig. 6a) a major discontinuity in frequency (staging) occurs at $M_j = 0.86$, where the tone jumps from 4.3 to 3.3 kHz. For the larger standoff distance, $h/D = 3.2$ (Fig. 6b), the frequency of the tone is rather insensitive to the change in the Mach number and remains almost constant at 3.7 kHz, except for $0.89 \leq M_j \leq 0.91$ where the majority of the energy appears to shift to the first harmonic, $f \approx 7.2$ kHz. The reason for such anomalous behavior is presently unknown.

In Figs. 6a and 6b some of the data points are circled. These data points represent the baseline cases that are used for the studies of impingement tone suppression. These figures also show a horizontal line representing the "resonant acoustic frequency." The resonant acoustic frequency is the full wavelength acoustic frequency that is calculated based on the standoff distance between the lift plate and the ground plate. For the standoff distance of $h/D = 2.4$ and 3.2 the resonant acoustic frequencies are 4465 and 3349 Hz, respectively. As will be discussed later, the proximity of the resonant frequency to the impingement tone frequency plays an important role in determining the effectiveness of the PRTs in suppression of the impingement tone.

Figure 7 shows the variation in the amplitude of the impingement tone (tonal amplitude) and the OASPL for the corresponding data points shown in Fig. 6. One can see that both the tonal amplitude and the OASPL rise gradually as the Mach number is increased. Further, there is no associated change in levels observed, when the jump in frequency is seen to occur.

B. Impingement Tone Suppression

The suppression of the impingement tone using the PRTs is examined next. The excitation frequencies selected for investigation in the present work are 10, 12, 14, and 17.5 kHz. The different excitation frequencies are generated by adjusting the depth of the resonance tube by means of the piston, as shown in Fig. 3. The resonance frequency is also a weak function of the NPR. Therefore, the nominal resonance frequency is specified by setting the depth of the resonance tube for a specific NPR. These are NPR = 1.63 ($M_{\mathrm{PRT}} = 0.865$) for 10 kHz, NPR = 2.04 ($M_{\mathrm{PRT}} = 1.063$) for 12 kHz, NPR = 2.72 ($M_{\mathrm{PRT}} = 1.286$) for 14 kHz, and NPR = 4.29 ($M_{\mathrm{PRT}} = 1.606$) for 17.5 kHz. Because the PRT produces tones using high speed jets the added mass flow is expected to provide fluidic excitation. To distinguish the acoustic excitation from the possible fluidic excitation, in the experiments described below, the PRT with zero depth is also examined. Note that this case did not produce any distinct acoustic tone.

Figure 8 shows characteristics of the PRTs for different nominal frequency settings, as the PRT jet flow varies with the NPR. Figure 8a

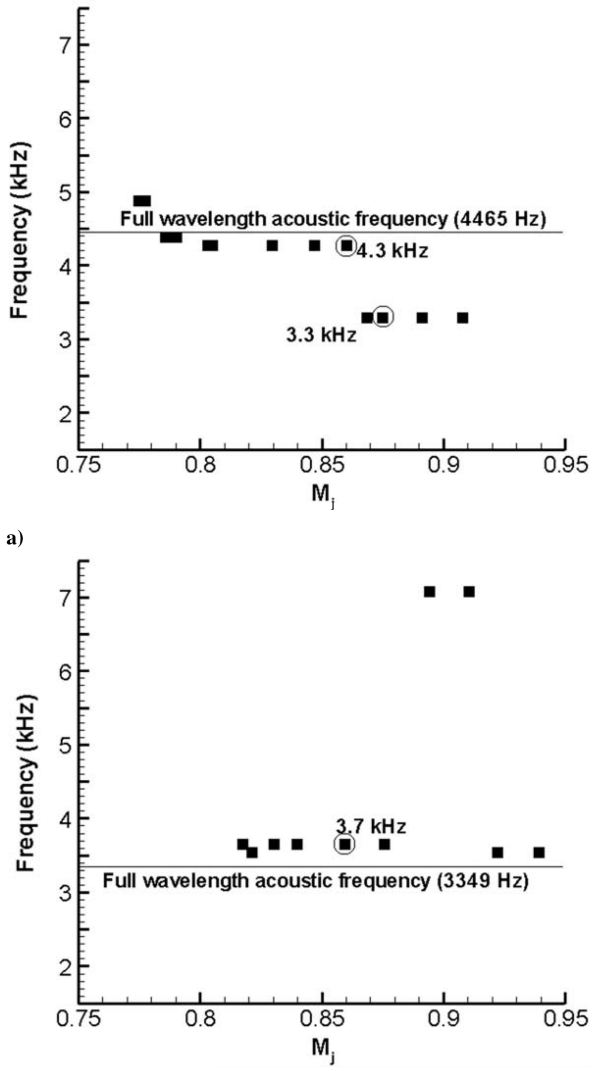

Fig. 6 Variation of the impingement tone frequency with jet Mach number. a) $h/D = 2.4$ and b) $h/D = 3.2$.

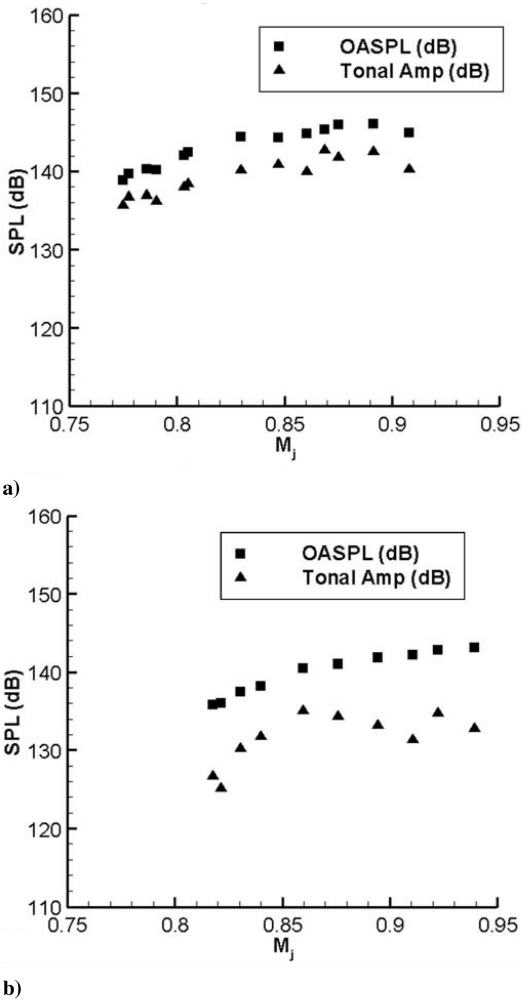

Fig. 7 Variation of the impingement tone amplitude and OASPL as a function of jet Mach number. a) $h/D = 2.4$ and b) $h/D = 3.2$.

shows that the PRT with relatively shallow depth tends to become NPR dependent, and its tonal frequency is found to monotonically decrease with increasing mass flow rate from the PRT. However, nominal frequencies of the PRTs with larger depth are seen to remain nearly constant with change in NPR. As the zero depth PRT (i.e., the fluidic excitation condition) does not generate any strong tone, this case is not shown. Figure 8b shows the variation in the amplitude of the resonant tone with NPR. As compared to the variation in the nominal frequency, the variation in the tonal SPL with NPR is appreciably large. Initially at lower NPR, the nominal frequency of the PRT and its corresponding tonal SPL are seen to have an inverse relationship—a tone with lower frequency has higher amplitude. However, with increasing NPR, the PRT tones of various nominal frequencies tend to reach the same maximum SPL (approximately 135 dB). For the zero depth PRT (fluidic excitation condition), the amplitudes are considerably lower than the acoustic excitation cases as expected, because effectively it is no longer a resonator tube.

The effect of high-frequency acoustic excitation on the primary[¶] impingement *tone* (here the tone implies a spike in the impingement

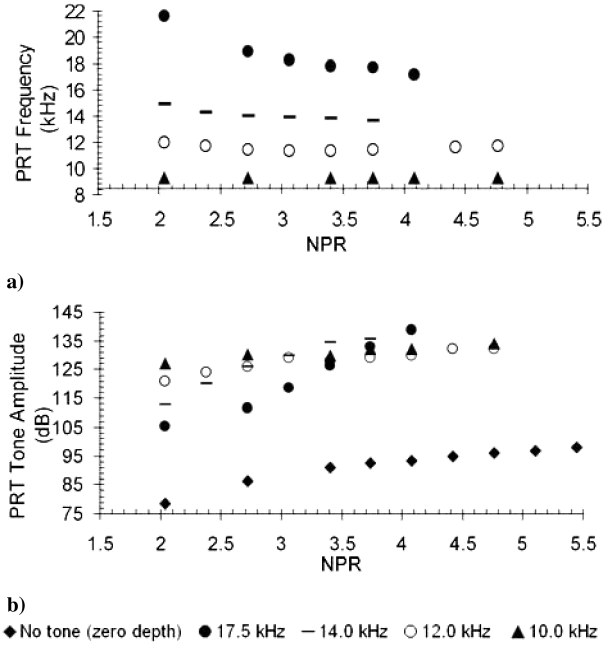

Fig. 8 Effect of NPR on the characteristics of the PRT. a) Tone frequency and b) tone amplitude.

[¶]When the impingement tone is suppressed, in certain cases, an additional tone/spike is observed (Fig. 11b). This additional spike/tone is referred to as the secondary impingement tone, whereas the original tone/spike in the spectra is referred to as the primary impingement tone. In the present paper whenever the impingement tone is referred to, it implies the primary tone, unless otherwise specified.

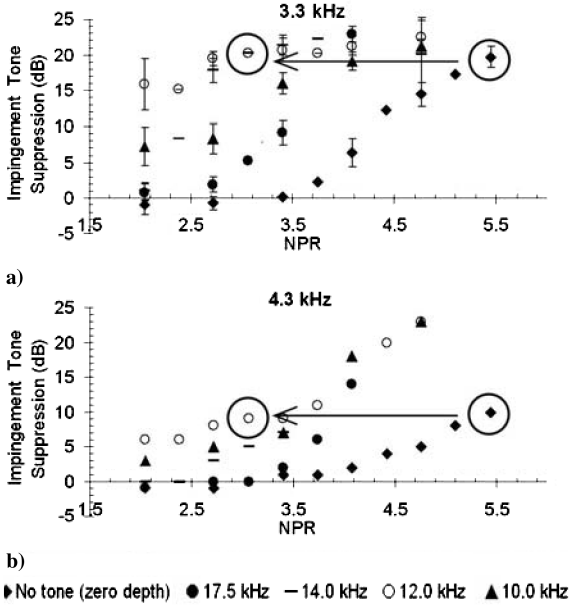

Fig. 9 Suppression of the impingement tone as a function of NPR for $h/D = 2.4$. a) $M_j = 0.88$ (resulting impingement tone occurs at 3.3 kHz) and b) $M_j = 0.86$ (resulting impingement tone occurs at 4.3 kHz).

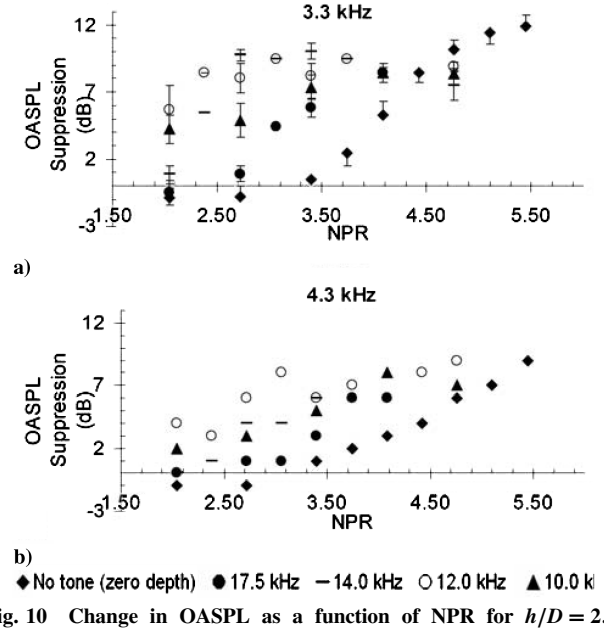

Fig. 10 Change in OASPL as a function of NPR for $h/D = 2.4$. a) $M_j = 0.88$ (resulting impingement tone occurs at 3.3 kHz) and b) $M_j = 0.86$ (resulting impingement tone occurs at 4.3 kHz).

tone spectra) is examined in Fig. 9. The suppression of the impingement tone for two jet Mach numbers, $M_j = 0.86$ and 0.88, at a standoff distance of $h/D = 2.4$, is examined. In the case $M_j = 0.86$ the impingement tone has a frequency of 4.3 kHz, and in the case $M_j = 0.88$ the tone has a frequency of 3.3 kHz. The suppression in the impingement tone is the difference in SPL without and with excitation, measured at the impingement tone frequency. A negative value in the graph is indicative of an increase in the amplitude when the PRTs are turned on. Figure 9a refers to the 3.3 kHz impingement tone, whereas Fig. 9b refers to the 4.3 kHz impingement tone. At first glance, the conditions leading to PRT resonant tones with higher SPL (Fig. 8b) are seen to be favorable in effective suppression of the jet impingement tone. However, a closer examination is made to evaluate the PRTs for the near optimum conditions. First we consider the impingement tone of 3.3 kHz frequency at $M_j = 0.88$ (Fig. 9a) and select the conditions when the PRTs with different resonant frequencies produce the same tonal SPL. That seems to happen for NPR = 2.7 and 3.4 in Fig. 8b, when the PRT tonal SPL reaches nearly 130 dB (within about 4 dB) except for the tone at 17.5 kHz which registers an SPL of about 110 dB for NPR = 2.7. For these cases, we note from Fig. 9a that the PRTs with 12 and 14 kHz tones result in the maximum impingement tone suppression of about 20 dB. The higher frequency PRT tones are not as effective, but at sufficiently high NPR (>4.1) they become equally effective. Further, we observe that the fluidic excitation is also effective in suppressing the impingement tone but requires much higher NPR. In fact, the fluidic excitation is seen to initially increase the impingement tone levels marginally and then start functioning effectively only beyond NPR = 3.4. A similar trend is observed in the case of the impingement tone frequency of 4.3 kHz obtained at $M_j = 0.86$ (Fig. 9b). Here, the PRTs become effective only when their flow rates reach a sufficiently high value (NPR > 4). Even the effect of the fluidic excitation is seen to be subdued. It is interesting to note that over the entire range of NPR used in the present study, the PRT tone with 12 kHz nominal frequency is consistently more effective than other frequencies for both the 3.3 and the 4.3 kHz impingement tones. The reason for diminished effectiveness of the PRTs in the suppression of the 4.3 kHz impingement tone is its proximity to the acoustic frequency based on the standoff distance. Similar observations were made in the case of the 3.7 kHz impingement tone (Fig. 6b) observed at a standoff distance of $h/D = 3.2$, where the acoustic frequency and the impingement tone frequency match occurred.

In both Figs. 9a and 9b, two of the data points are circled. They represent nearly equal suppression of the impingement tone, one achieved through purely fluidic excitation (the PRT set at zero depth) and the other through a 12 kHz acoustic excitation. The difference between the two data points is the NPR at which the suppression is obtained. The suppression with the fluidic excitation is achieved at an NPR of 5.4, whereas the acoustic excitation yields a comparable suppression level at a reduced NPR of 3. This reduction in the NPR at which the PRT operates translates to a reduction in the mass flow rate by about 45%, which means substantial energy savings. Thus in comparison with the pure fluidic excitation, the high-frequency acoustic excitation is a more effective strategy for suppressing impingement tones. Here it is important to point out that even at the maximum NPR attempted in the present experiments, the net mass flow from all four PRTs is of the order of 2% of the main jet's mass flow rate.

Figure 10 shows attenuation of OASPL as a function of the NPR. It can be observed that SPL of the PRTs increases with NPR. Note, however, that the impingement tone amplitude remains constant for each part (Figs. 10a and 10b). The net result is a reduction of 9–11 dB in the overall noise level achieved from the addition of noises from the PRT and the impinging jet.

Although the OASPL is a good measure of the total energy contained in the acoustic spectrum, it is not indicative of human annoyance to the noise. In the aircraft industry the perceived noise level corrected for the tone (PNLT) is used as a measure of sound that characterizes the degree of human annoyance. As per the PNLT analysis the annoyance level of sound depends on its frequency content. The sound which lies in the frequency zone of 1–5 kHz is considered to be the most annoying, hence penalized heavily, whereas the frequency content of the sound which lies above 5 kHz is considered to be the least annoying, hence receiving less penalty.

Table 1 summarizes the results of the OASPL suppression and the PNLT suppression obtained with the PRT tone of 17.5 kHz nominal

Table 1 Comparison between the PNLT suppression and the OASPL suppression. Impingement tone frequency: 4.3 kHz; frequency of the PRT resonant tone: 17.5 kHz

NPR	PRT amplitude, dB	Impingement tone suppression, dB	OASPL suppression, dB	PNLT suppression, dB
3.74	133	6	6	8
4.08	139	14	6	12

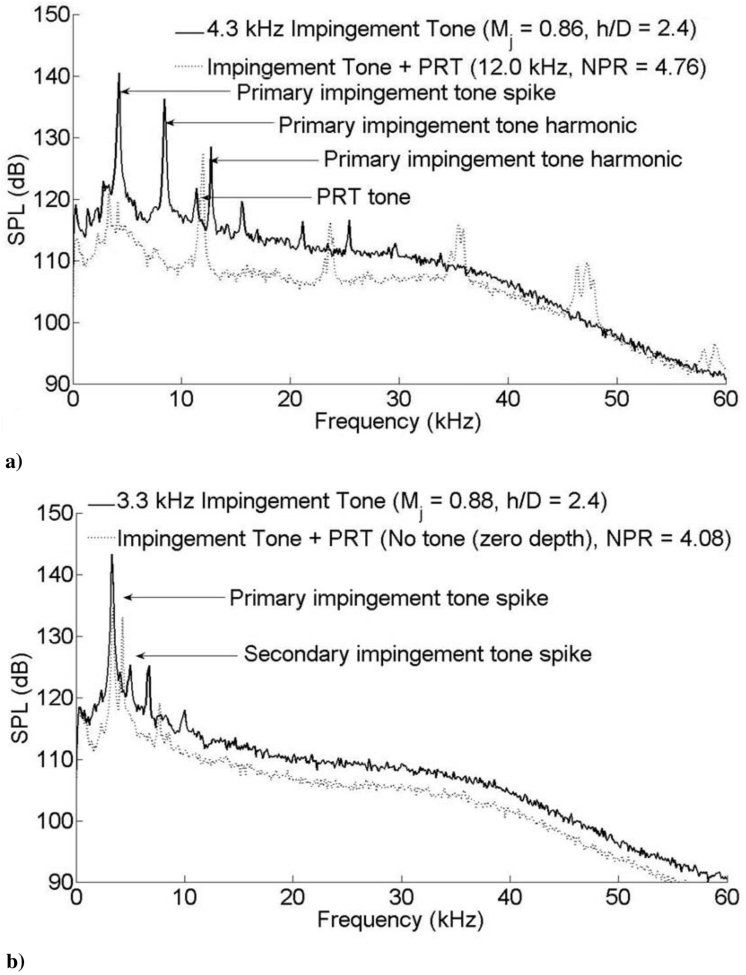

Fig. 11 Impingement jet noise spectra for $h/D = 2.4$. a) $M_j = 0.86$, solid line: PRT off; dashed line: PRT actuating at 12 kHz. b) $M_j = 0.88$, solid line: PRT off; dashed line: PRT actuating at NPR = 4.08 without any tone (zero depth).

frequency at two different NPRs, viz., 3.74 and 4.08. It can be seen that increasing the NPR from 3.74 to 4.08, the impingement tone suppression is increased by 8 dB. However, the increase in NPR also increases the amplitude of the PRT tone by 6 dB, from 133 dB at NPR = 3.74 to 139 dB at NPR = 4.08. Thus the effect of increase in the impingement tone suppression at higher NPR is leveled off by additional noise from the PRTs, resulting in unchanged OASPL. However, because the PRT tone lies in the frequency range of 5–20 kHz, for which there is less penalty, the PNLT suppression level is improved by 4 dB. Hence it can be said that, even though the suppression of the impingement tone may be offset by the addition of the noise from the PRT, the acoustic excitation provided by the PRTs invariably reduces the *annoyance* level of the impingement tone.

Figure 11 shows spectra at two slightly different Mach numbers with and without PRT excitation. These Mach numbers (0.86, 0.88) produce a dominant impingement tone at 4.3 and 3.3 kHz, respectively. Comparison of Figs. 11a and 11b reveals the distinct nature of the 4.3 and the 3.3 kHz impingement tones. The 4.3 kHz impingement tone, which is very close to the resonant acoustic frequency, is dominated by the first few harmonics, whereas the 3.3 kHz spectrum contains only the first harmonic and a few additional nonharmonic peaks, which are weak in strength. The spectra of the corresponding cases when suppressed using PRTs also showed distinctive results. In the case of the 3.3 kHz spectrum (Fig. 11a) turning on the PRTs gives rise to an additional spike—referred to as secondary tone—at 4.3 kHz. The degree of the augmentation of this secondary tone depends on the particular PRT setting and the primary impingement tone suppression. Such additional spikes are not observed during the suppression of 4.3 kHz impingement tone case.

IV. Conclusions

The present work explored the suppression of impingement tones using PRT actuators. The work began by characterizing staging behavior of the impingement tone produced by the main nozzle for various Mach numbers and standoff distances. Next, we used PRTs to introduce high-frequency excitation in the transitional region of the shear layer of the main jet. The tonal amplitude, OASPL, and PNLT suppression levels were examined for various actuation conditions (frequency, amplitude, and mass flow rate) at different impingement tone frequencies.

The following important results emerged from this study:

1) The PRT actuator was capable of suppressing tonal SPL, OASPL, and PNLT of the impinging jet from the main nozzle. Tonal suppression levels were as high as 20 dB with less than 2% mass addition. The corresponding OASPL suppression levels ranged from 5 to 10 dB.

2) We observed that the impingement tone could be suppressed either by a strongly resonating PRT or a zero depth PRT (with no dominant tone), both of which were sources of unsteady mass addition. However, the mass flow requirements were substantially lower for the former.

3) It was found that impingement tones that matched the full wavelength acoustic frequency ($h = \lambda$) were more difficult to suppress.

Acknowledgement

This work has been carried out under the support of the U.S. Air Force Office of Scientific Research (AFOSR) Small Business Technology Transfer Program (STTR) Phase II Contract No.

F49620-02-C-0098. John Schmisseur served as the AFOSR Program Manager.

References

[1] Tam, C. K. W., and Ahuja, K. K., "Theoretical Model of Discrete Tone Generation by Impinging Jets," *Journal of Fluid Mechanics*, Vol. 214, May 1990, pp. 67–87.

[2] Masuda, W., and Nakamura, T., "A Feasibility on Aerodynamic Characteristics of Underexpanded Annular Impinging Jets for Assisting Laser Cutting," *Proceedings of an International Conference on Laser Advanced Materials Processing (LAMP'92)*, Nagoaka, 1992, pp. 613–654.

[3] Aratani, S., Narayanswami, N., Ojma, H., and Takayama, K., "Studies of Supersonic Jets and Shock Waves Generated During Glass Tempering Process," *Transaction of the Japan Society of Mechanical Engineers (B)*, Vol. 61, No. 590, 1995, pp. 1277–1282.

[4] Krothapalli, A., Rajakuperan, E., Alvi, F. S., and Lourenco, L., "Flow Field and Noise Characteristics of Supersonic Impinging Jet," *Journal of Fluid Mechanics*, Vol. 392, Aug. 1999, pp. 155–181.

[5] Sheplak, M., and Spina, E. F., "Control of High Speed Impinging Jet Resonance," *AIAA Journal*, Vol. 32, No. 8, 1994, pp. 1583–1588.

[6] Alvi, F. S., Shih, C., Elavarasan, R., Garg, G., and Krothapalli, A., "Control of Supersonic Impinging Jet Flows Using Supersonic Microjets," *AIAA Journal*, Vol. 41, No. 7, 2003, pp. 1347–1362.

[7] Cain, A. B., Rogers, M. M., Kibens, V., and Raman, G., "Simulation of Frequency Excitation of a Plane Wake," AIAA Paper 2001-0514, Jan. 2001.

[8] Kral, L., "Active Flow Control Technology," *American Society of Mechanical Engineers Technical Brief*, 1999.

[9] Wiltse, J. M., and Glezer, A., "Direct Excitation of Small-Scale Motions in Free Shear Flows," *Physics of Fluids*, Vol. 10, No. 8, 1998, pp. 2026–2036.

[10] Cain, A. B., Rogers, M. M., and Kibens, V., "Characterization of High Frequency Excitation of a Wake by Simulation," AIAA Paper 2003-0179, Jan. 2003.

[11] Hartmann, J., and Troll, B., "On a New Method on the Generation of the Sound Waves," *Physics Review*, Vol. 20, 1922, pp. 719–727.

[12] Brocher, E., Maresca, C., and Bournay, M. H., "Fluid Dynamics of the Resonant Tube," *Journal of Fluid Mechanics*, Vol. 43, No. 2, 1970, pp. 369–384.

[13] Raman, G., Khanafseh, S., Cain, A. B., and Kerchen, E., "Development of High Bandwidth Powered Resonance Tube Actuators With Feedback Control," *Journal of Sound and Vibration*, Vol. 269, Nos. 3–5, 2004, pp. 1031–1062.

[14] Powell, A., "On Edge Tones And Associated Phenomenon," *Acoustica*, Vol. 3, 1953, pp. 233–243.

[15] Murugappan, S., and Gutmark, E., "Parametric Study of the Hartmann–Sprenger Tube," *Experiments in Fluids*, Vol. 38, No. 6, 2005, pp. 813–823.

[16] Sarpotdar, S., Raman, G., and Cain, A. B., "Powered Resonance Tubes: Resonance Characteristics and Actuation Signal Directivity," *Experiments in Fluids*, Vol. 39, No. 6, 2005, pp. 1084–1095.

[17] Murugappan, S., and Gutmark, E., "Experimental and Computational Study of High Frequency Actuation of Supersonic Jets," AIAA Paper 2003-370, Jan. 2003.

[18] Kastner, J., Hileman, J, and Samimy, M., "Exploring High-Speed Axisymmetric Jet Noise Control Using Hartmann Tube Fluidic Actuators," AIAA Paper 2004-0186, Jan. 2004.

[19] Raman, G., and Kibens, V., "Active Flow Control Using Integrated Powered Resonance Tube Actuators," AIAA Paper 2001-3024, June 2001.

[20] Raman, G., Mills, A., and Kibens V., "Development of Powered Resonance-Tube Actuators for Aircraft Flow Control Applications," *Journal of Aircraft*, Vol. 41, No. 6, Nov./Dec. 2004, pp. 1306–1314.

[21] Raman, G., and Cain A. B., "Innovative Actuators for Active Flow and Noise Control," Proceedings of the Institution of Mechanical Engineers, Part G: *Journal of Aerospace Engineering*, Vol. 216, No. 6, 2002, pp. 303–324.

N. Chokani
Associate Editor